Nonlinearities in Loudspeaker Ports

John Vanderkooy
Audio Res. Group Univ. of Waterloo Canada

Presented at the 104th Convention 1998 May 16-19 Amsterdam

AN AUDIO ENGINEERING SOCIETY PREPRINT

Nonlinearities in Loudspeaker Ports

John Vanderkooy
Audio Research Group,
Dept of Physics
University of Waterloo,
Waterloo ON Canada N2L 3G1
<jv@audiolab.UWaterloo.ca>
Tel: 519-885-1211 x2223 Fax: 519-746-8115

Abstract

The increasing demand for high SPL at low frequencies has prompted this study of nonlinearities in loudspeaker ports. At high levels, ports produce jets of air, display acoustic compression, loss and distortion, generate turbulence noise, and rectify pressure fluctuations. These phenomena are measured and analyzed. A simplified nonlinear model of a port is presented. Flared ends and gentle tapering help somewhat. The low-level linear acoustic characteristics of ports of varying cross-section are analyzed. The velocity profiles of some ports are measured, and a new theory for this and the associated nearfield pressure is presented, which contradicts the usual "piston-in-a-baffle" approach.

Introduction

In an earlier paper some data on overdriven ports was presented, and a model of a tapered port was given [1]. This paper extends that work and presents an understanding of high-level phenomena in ports along with further corroborative experiments.

Systems without ports have a low-frequency efficiency that is a bit low to be practicable, so the resonant properties of a port and an associated volume of air are usually employed. Vented-box or reflex enclosures with ports have been analyzed by Thiele and Small. Subwoofers can also be designed with coupled-cavity configurations, in which the port is the sole source of the sound that emerges. As sound levels rise, the air velocity in the port increases, until ultimately there is too much distortion, compression, or aerodynamic noise from the port. The passive radiator is an alternative to a simple port, and has some advantages, but it is more costly. Ports are thus expected to remain in use, and the purpose of this paper is to study their operation at high levels.

There has been an extensive study by Backman [2], which presents measurements of some interesting configurations, and the compression which occurs at high levels, but the focus of the study is not a detailed understanding of the underlying mechanisms. A much earlier acoustic study of a small orifice [3] does give some details of the processes involved, and we build on these results. For high levels, it shows that the velocity at the orifice opening roughly relates to the pressure, p, driving it, by:

$$p = (\text{air\_density}/2)*(\text{air\_velocity})^2.$$

For ports, we thus might naively expect a significant second-harmonic generation, but this does not happen. However, the major compression characteristics of ports are explained by this concept.

Theory for the linear behaviour of ports is presented, and a model for a port of varying cross-section is analyzed. Measurements agree fairly well with the model at low levels.

The nonlinear aspects of ports are analyzed and a simple model is proposed. Ports of various diameters and lengths are studied, and tapered ports and flared ends are considered. These latter show a lower tendency to produce jet flow and thus display somewhat less compression.

Measurements have led to an understanding of the sound field and airflow pattern in the nearfield, the circulation of air near the port due to inertial jet flow, and rectification of the flow pattern. Many of the features of the airflow near ports, and its effect on microphone measurements, have been elucidated in a companion paper [4]. At a certain critical velocity, the flow is unstable against jet formation. The airflow near a transducer is itself modified so that the outward velocity is larger near the axis (i.e. the flow forms a jet), while the inward velocity is more or less hemispherically directed. The distortion is severe and compression takes place as the acoustic effects are dominated by the inertial effects of the flow.

Ports which have asymmetry in the flow may produce a static pressure difference between the inside and outside of a loudspeaker box. This may cause cone offset with attendant deleterious effects. An example of a static pressure difference was given in [1].

Experimental Setup

The ports under test were mounted on a 25-l box, which was driven by a large driver from the back, as shown in Fig.1. One driver used was an 18-inch woofer with a 4-inch voice coil in a relatively short strong magnetic gap, hence it is efficient with plenty of available volume velocity. The other driver was a 12-inch very long-throw unit with a large magnet structure having a long gap, and a short voice coil. This driver has reasonable damping and although of somewhat lower maximum volume velocity, it has a smaller cone area and is capable of higher box pressure when loaded with smaller ports.

Typically, ports were flush-mounted on a large 4 x 4-ft. baffle, which was attached to the front of the box. In this way a pair of close microphones (typically 10-20 cm away) can assess solely the output from the port, with no contamination from the rear-mounted driver. Other double-flanged and usually symmetric ports were bolted to the front of the box, and heavy cardboard baffling was affixed to the protruding port, again allowing an assessment of only the sound from the port. When the port outputs were blocked with rubber stoppers, the sound level at the microphones outside the box would fall by over 30 dB, indicating that the sound from the driver coming around the baffle was negligible.

A low-distortion oscillator feeding a 160W/Ch power amplifier was used to drive the system, and the current to the driver was monitored with a 0.1-ohm series resistor. Most experiments were carried ou at 30 Hz, this being judged representative of actual use. A 1/4-inch B&K type 4135 microphone was mounted in one side wall of the box to monitor the driving pressure. Several B&K type 4133 microphones were used to measure the output from the port. Although these are free-field microphones, they have essentially a pressure response below 5 kHz.

Two dual-channel data acquisition cards with programmable anti-aliasing filters were used to capture four simultaneous channels of information. The sampling frequency was usually 5 kHz with the filters set near 1 kHz, and time records were 4096 samples long. Results were analyzed in both time and frequency domains. Most of the interesting signals and noises from the ports are well below 1 kHz. Time signals best show the nature of the measurement errors, when they are severe. Spectra of the time signals were derived by 4096-point DFTs with either a Hann window (for sharp peaks) or a 5-term flattop window (with very low scallop error for accurate peaks).

Pressure and Velocity Relationships at Low Levels

All the air that moves through a port must pass the throat, and for a compact source (size << wavelength) the retarded volume acceleration, A(t) [m^3/s], acts as the source of the external farfield pressure, p, at a distance, r, from the mouth, given for a baffled port by [5]:

$$p = \rho\, A(t-r/c) / (2\,\pi\, r). \tag{1}$$

If V_0 is the velocity amplitude in the throat of area A_0 at angular frequency ω, then the volume acceleration is $A_0\, j\, \omega\, V_0$, leading the velocity by 90 degrees. Thus a measure of the sound pressure at a specific distance from the mouth allows us to obtain the throat velocity using the relation:

$$V_0 = 2\,\pi\, r\, p / (j\, \omega\, \rho\, A_0). \tag{2}$$

The pressure inside a loudspeaker box also bears a straightforward relationship to the velocity in the port and also to the farfield pressure outside the box created by the port. Our basic premise is that the pressure outside the box is essentially negligible relative to the pressure in the box. We justify this later.

Fig.2 shows a box with inside pressure, P, throat velocity, v, with port area, A_0, length, L, and farfield pressure, p, at radius, r. The acceleration, a, of the mass $M = \rho\, A_0\, L$ of air in the port acted on by a force $F = P\, A_0$ is:

$$a = P\, A_0 / (\rho\, A_0\, L) = P / (\rho\, L) \tag{3}$$

which does not depend on the throat area. Since the amplitudes of acceleration and velocity are related as $a=j\omega v$, where ω is the angular velocity, the velocity in the port is given by:

$$v = P / (j\, \omega\, \rho\, L). \tag{4}$$

The volume acceleration, A_0 a, is the source for the farfield pressure as discussed earlier, and since the acceleration is directly proportional to the pressure P from (3), we have for a baffled port opening

$$p = (A_0 / L)\, P / (2\,\pi\, r). \tag{5}$$

Aside from the distance factor, the A_0 / L ratio of the port enters directly, and the outside pressure is (apart from retardation) exactly in phase with the box pressure.

It remains to justify that we can set the pressure outside the box to zero in our theory. We have so far ignored the end corrections for the reactive radiation load on the two ends of the port. It is precisely

these which take into account the pressure required to move the air at the ends. If we use the full effective length of the port, including the end corrections, then the theory above works essentially with full box pressure at the port inner entrance and zero pressure at the equivalent port mouth, except for a very small resistive component of the radiation load, which really is negligible at bass frequencies with typical port diameters.

The Linear Acoustic Behaviour of Ports of Varying Cross-section

We first review the resonance properties of a standard port consisting of a normal, cylindrical tube of cross-sectional area, A, and length, L, which is coupled to a box of volume, V. The mass, M, of the air in such a port is:

$$M = \rho A L \tag{6}$$

where, ρ, is the density of the air. If the "plug" of incompressible air in the port moves out a small distance, dx, the volume change, dV is

$$dV = A\, dx \tag{7}$$

and the pressure change across the port for an adiabatic process (no heat transfer) is

$$dP = -\gamma P_0\, dV / V = -\gamma P_0\, A\, dx / V, \tag{8}$$

where P_0 is atmospheric pressure and $\gamma = 7/5$ for air. The force dF on the air plug is

$$dF = A\, dP = -\gamma P_0\, A^2\, dx / V, \tag{9}$$

so from dF=-k dx the spring constant k of the air in the volume V is

$$k = \gamma P_0\, A^2 / V. \tag{10}$$

With the mass M given above in (6), the resonance angular frequency ω of this mass-spring combination is given by

$$\omega^2 = \gamma P_0\, A / (\rho\, V\, L). \tag{11}$$

Note that the squared resonance frequency depends on the A/L ratio of the port. A more complete analysis yields reactive radiation end corrections to L: for a baffled end, we must add a length of 0.85 R, and for a free end, 0.61 R, where R is the port radius [6].

If a port has a varying cross-sectional area, the analysis must proceed along different lines, since the air cannot be regarded as a simple cylindrical plug. The pressure change through the port is calculated by considering the contributions of thin sections perpendicular to the port axis.

Assume that a displacement X_0 of the air occurs at the neck of the port, at angular frequency ω. If the neck cross-sectional area is A_0, then the volume of air that has passed the neck is $A_0\, X_0$. For the purpose of dealing with this lumped acoustic element, we consider the air as incompressible, thus the same volume must pass through any transverse section. Therefore the amplitude at position x is

$X_0 A_0/A(x)$, where A(x) is the cross-sectional area at position x. The acceleration will be $-\omega^2$ times this value. If ρ is the density of the air, the pressure change, dp, to accelerate a thin disk of air of thickness, dx, will be

$$dp = -\rho\, \omega^2\, X_0\, dx\, A_0/A(x), \tag{12}$$

and to obtain the total pressure we integrate along the axis of the port, giving

$$p = -\rho\, \omega^2\, X_0\, A_0 \int (dx/A(x)). \tag{13}$$

The amount of air that flows through the throat of the port is $A_0\, X_0$, so the pressure change in the volume V is $-\gamma\, P_0\, A_0\, X_0/V$, where P_0 is atmospheric pressure. Equating this pressure change to that of the integral above, the resonance angular frequency ω becomes:

$$\omega^2 = \gamma\, P_0\, /(\rho\, V \int (dx/A(x)). \tag{14}$$

The properties of the port occur only in the integral. The resonance frequency of a cylindrical port depends on the A/L ratio of the port. Comparing (11) and (14), we see that the equivalent A/L for a general port is

$$A/L = 1\, /\, \int (dx/A(x)). \tag{15}$$

There are a number of caveats in this derivation. It is assumed that the area function A(x) is such that the integral defined above is finite. This means that as |x| increases, A(x) must decrease faster than 1/|x|, or else the effective mass of the air in the port becomes infinite. If the shape of the port is flanged or has an open end, then the integral must be augmented respectively by end corrections such as 0.61 Re/Ae or 0.85 Re/Ae, where Re and Ae represent the radius and area of the end of the port.

As an example, consider a symmetrical port with a gentle flare whose cross-sectional area as a function of distance x along its axis is

$$A(x) = A_0 \cosh(x/l), \tag{16}$$

where A_0 is the area at the neck or throat, and l is the scale length of the flare. A real port might use this shape near the middle, but would smoothly "connect" it to the flat baffle of the speaker exterior. Nevertheless, acoustically the shape defined above is the relevant one, because the motion of the air becomes smaller and less important as the area increases. The varying area acts as a mechanical transformer to reduce the inertial effects of the air in the wider sections of the port where the velocity is lower.

The effective A/L value of such a port is easily computed since the integral in (15) is easily evaluated for a hyperbolic cosine, giving

$$A/L = A_0/(\pi\, l). \tag{17}$$

Thus the effective length of this port is π l, if we use the neck as the area reference.

A port of shape given by (16) was constructed of fiberglass and tested to determine the resonance frequency when it was mounted on a closed box. This symmetrical port had a scale length l=3.85cm, a neck diameter of 4cm, and a total length of 18cm with flanged ends. The box volume was 2.3 litres and the resonance frequency was measured to be 110Hz. A careful calculation of the integral over the finite length of the port, with end corrections, gives an A/L value of 0.0102 m. This results in a resonance frequency of 115Hz, which is regarded as good agreement with theory.

A possibly significant modification to the theory above is to consider that the air motion in the port must conform to the walls of the port. Hence the lines of constant displacement in the port will tend to have a curved shape. The cross-sectional area will be less than the intercept of the plane perpendicular to the axis at the relevant value of x. This reduces A(x) somewhat, thereby reducing the effective A/L value. Our values of the resonance frequency measured above indicate that this effect has the wrong sign to explain the small discrepancy between theory and experiment. We return to the discrepancy between resonance frequencies later...

Measurements of Flow Velocity and Formation of a Jet

In order to study the airflow near a port, a hot-wire anemometer probe was constructed. An 8 mm length of #44 copper wire was soldered between two parallel pointed copper rods 3 mm in diameter. A plot of voltage versus current for the probe showed that the resistance at 1.0 A was 1.57 times that at room temperature. Since the resistance of a pure metal such as copper is closely proportional to the absolute temperature [273 + T(C)], the wire was about 190C at 1.0 A.

The wire was driven by a power op-amp in a Wheatstone-bridge feedback configuration, which maintained the wire at constant resistance, and hence constant temperature. This removes the thermal inertia of the wire from the response characteristic and results in very rapid response, to fractions of a millisecond. The wire loses heat by forced convection due to air flow, and the change in bridge driving voltage is closely proportional to the square root of the air velocity. A squaring circuit applied to the change of bridge voltage then gives a signal representing the air velocity. The probe is sensitive only to air speed, not direction, for motion perpendicular to the wire. It was found difficult to make the system properly stable, so the anemometer shows some output fluctuations, which may not represent actual air velocity changes.

Calibration of the hot-wire anemometer was done with a specially-constructed nozzle, driven by an air supply with a pressure measured by a reference water manometer. For the probe described, the air speed was 4.69 m/s for 1 volt of output.

Fig.3 shows four signals, respectively from a pressure microphone in the box (a), the output of a microphone outside the box on the baffle 10cm from the port (b), another mounted 20 cm from the port, also on the baffle (c), and the output of the hot-wire anemometer (d) whose probe was placed in the centre of the port in the baffle. The port is 7.5 cm in diameter, cut into a baffle 1.7 cm thick. The frequency of the excitation to the driving loudspeaker is 30 Hz, and the level of the sound is low enough that no appreciable inertial effects occur. The air flow is purely acoustic. Note that the box pressure causes an air velocity that is lagging the pressure by 90 degrees. The peaks in the air velocity labelled by "O" represent outwardly-flowing air, and those labelled by "I", inwardly-flowing air. The signal appears to be frequency doubled since the anemometer responds only to the magnitude of the air speed, not its direction.

Note that the acoustic pressure outside the port is in phase with the box pressure, in agreement with earlier theory. The pressure outside the box is in phase with the acceleration of the air in the port, which in turn is in phase with the box driving pressure, as indicated by earlier theory.

Fig.4 shows the same four signals as earlier, but with 20 times the drive to the loudspeaker, and the hot-wire probe has been placed 10cm in front of the hole. Its output, (d), is consistent with a jet of air issuing from the port in a narrow column. The peak air velocity is just over 20 m/s. There is a delay in the arrival time of the velocity peak, due to the travel time of the moving air. The nearer microphone, (b), responds to the volume acceleration of the air from the port, and displays distortion and a phase lag due to the velocity-related losses in the port. The farther microphone, (c), also shows distortion, but this signal better represents the pressure, and does not change shape with further distance.

Fig.5 shows the signals of Fig.4 (b) and (c) normalized to similar amplitude. The nearer pressure signal seems contaminated by a component that occurs at the peaks of the velocity shown in Fig.4(d). The distortion is largely positive, whereas a Bernoulli effect would predict a negative component.

For negative box pressures the air outside comes in radially with much less velocity, and thus the air speed signal displays strong asymmetry, but remember that the jet of air is now being formed inside the box. The flow, while distorted from a pure sine wave, has odd symmetry which causes odd-order distortion of the pressure signal in the box, Fig.4(a), and of the external pressure, Fig.4(c).

Fig.6 shows measurements of the air velocity at distances of 1, 2, 3, 5, 10, 15, 20, 30 and 50cm along the axis of the port. By following the progress of a velocity peak from 0 to 30 cm from the port, the translational speed of the velocity peak works out to about 10 m/s. However, the peak velocity is about 20 m/s! This means that whatever is moving is not simple. The literature on fluid mechanics indicates that an orifice, when in the blowing phase, may shed a vortex ring, which propagates at a lower speed than the air in the centre of it. That may explain why the velocity peaks are rather sharp, even though the port is blowing out 50% of the time. By 50cm, the jet is beginning to dissipate. Fig.7 shows longer time records of the air velocity at 50 and 80cm from the port illustrating the chaotic nature of the air flow, which now has reduced speeds..

The formation of the jet by a port is complex, and although a number of experiments were done to come to some general conclusions, a final determination of the conditions and jet characteristics will be the subject of future investigations. Broadly, for the conditions of the ports studied here, the flow velocity is usually between 5 to 10 m/s when instability occurs. This corresponds to a Reynolds number of 25000 to 50000 for a port of 7.5-cm diameter. Flared ends and/or gentle tapers increase somewhat the throat velocities before jet formation. The smoothness of the port surfaces may also affect the onset of instability. More details of the jet and its measurement are given in [4].

The jet itself is rather tenuous, and it is significantly altered or deflected by obstacles which prevent the formation of vortex rings at the mouth of the port. These obstacles probably do not significantly alter the acoustical properties, which are dependent on the local pressure and flow at the port. The jet is an inertial effect of the air projected from the port, and it has no effect on the efflux of the air once it has passed the throat of the port. The kinetic energy of this air has already been lost to the acoustic system, and will be dissipated thermally nearby.

As the excitation to the driver on the box is increased, fluctuations of the current can be observed, probably due to the varying pressure conditions at the port. The anemometer shows wild fluctuations at the same time, presumably due to local changes in air speed and/or direction. It is as if puffs of air cannot quite decide in which direction to go, and this can be felt by the hand held near the port. For higher excitation, these nearby fluctuations disappear, presumably because the flow pattern, though now turbulent at smaller scales in both distance and time, is nonetheless in steady state with respect to an excitation period. However, when the hand is held further out, in the range where the jet is dissipating, slower fluctuations can again be felt.

Another surprising observation was a hysteresis effect. For a 7.5-cm port 10 cm long, the critical driving current was 0.53 A before instability set in, as measured by the anemometer mounted a diameter away on axis. The transition was quite sharp. Once unstable and producing chaotic airflow, the port did not return to a stable acoustic flow until the excitation was reduced below 0.40 A. While one might have expected such behaviour when a steady flow is varied, this hysteretic effect occurs at 30 Hz, so the flow conditions are continually changing and reversing. The existence of hysteresis means that the system must have a memory of its past. Thus we surmise that the chaotic or streaming flow away from the port mouth must affect the next cycle as well, to retain unstable behaviour until the excitation is reduced below yet another threshold.

A Nonlinear Port Model

In order to understand better the output of a port when highly overdriven, a somewhat simplistic but tractable model was constructed which takes into account the major features of the air flow. Inspiration for this model comes from [3]. The main addition to the simple acceleration model outlined in (6)-(17) is that when velocities are high, the air in the throat forms a jet, which moves as a column into the surrounding open area, and we can apply conservation of energy to this flow pattern. The energy from this jet will ultimately be dissipated by eddies due to viscosity of the air, and does not concern us, since these processes do not result in acoustic sources of consequence unless microphones are placed very close to these eddies, which radiate as quadrupoles.

Thus we consider a steady-state situation in which air at pressure p in the box flows toward a hole and accelerates till it reaches the throat. The Bernoulli theorem applies to such lossless flow and we find for the magnitude of the velocity (assumed constant across the port, about which more later)

$$\rho v^2 / 2 = p, \tag{18}$$

We modify the equation above to

$$\rho v |v| /2 = p, \tag{19}$$

so that the sign of v is rendered correctly, since the pressure in the box will be oscillatory. In normal acoustic flow, the air leaving the port will again slow down as it spreads out, and there will be no jet, and hence no lossy pressure term as given by (18).

However, since the flow is not steady, we will add an additional term to accelerate the mass of the air in the port as well. For a port of length l, the acceleration of the air is the derivative of velocity, and from Newton's law we have

$$\rho\, l\, dv/dt = p. \qquad (20)$$

The model is somewhat artificial in that each process involves Newton's law, but we regard (19) as due to a loss mechanism (which leaves kinetic energy in a jet stream), whereas (20) relates to the lossless aspects. Finally then, adding the two pressure components above and setting them equal to the box pressure,

$$\rho\, l\, dv/dt + \rho\, v\, |v| /2 = p(t). \qquad (21)$$

Given the pressure p(t), this differential equation can easily be numerically integrated to find v(t). It is clear that at low pressure amplitudes, the v |v| term is negligible and we regain (20), whereas at very high amplitudes, the behaviour will approach that of (19).The length l in (20) and (21) should include end corrections to the port, being 0.85 R for a flanged end, and 0.61 R for an unflanged one.

To assess the above model, we apply it to the measured box pressure of Fig.4(a), and compare the measured outside pressure and velocity with model calculations. Fig.8 again shows the measured box pressure at 20cm along the baffle for the overdriven 7.5cm hole in a baffle 1.7cm thick (upper), and the calculated model outside pressure at 20 cm (lower). End corrections of 0.85 R have been applied to both ends. The curves do not agree well; the scales are reasonable but the detailed shapes are not.

It was noticed that as the excitation is increased, the onset of jet formation is very sudden and occurs for a critical velocity that is somewhat dependent on port size . When the air speed is sufficient to create a jet on the exit side, one should then remove that end correction, since the airflow does not spread out and stagnate as it should, and vice-versa for reversed flow. Also, the v |v| effects have a threshold below which there is no jet, and then they should not be applied at all, leaving only normal acceleration.

We can comply with these observations by switching on the v |v| term only above the critical velocity, at the same time removing the end correction for the appropriate side. Any discontinuities in the outside model pressure due to sudden changes in acceleration are smoothed by including a gentle switching transition.

After these additions to the program, the calculated outside pressure improved only marginally, and although the shapes could be made slightly better, the model was still deficient. However, there is sufficient conformity to reality that we regard the model study as useful to corroborate the basic effects of the jet flow and the modified end corrections. The next section deals with a complexity which may partially explain the inability of the model to conform well to the measurements.

Velocity Profile and Nearfield Pressure of a Port

The velocity profile across a port is often assumed to be uniform. The acoustic output can then be calculated by the Huygens-Rayleigh integral under a second common assumption, that the port exhausts into an infinite baffle. These familiar "piston-in-a-baffle" results are widely used, and for a driver they apply rather well. In reality of course, the speaker box further modifies the acoustic output of both driver and port, and although estimates could be made of the 2π to 4π transition, the proximity of room surfaces complicates things further, so further calculations are seldom attempted.

The assumption of a uniform velocity profile turns out to be faulty for most ports. For both low- and high-level excitation, the velocity across a 7.5 cm port in a 1.7 cm-thick baffle was measured by a hot-wire anemometer. At low levels, the rms velocity versus distance from the centre of the port was measured at three points in the baffle plane. At distances of 0, 1, 2, and 3 cm from the centre, the velocities respectively were 0.725, 0.761, 0.965, and 1.17 m/s. This is well below the critical velocity of this port. The measurement near the edge shows increasing instability on the hot-wire probe, which may represent turbulence due to the shedding of eddies from the sharp inner edges of the port. The velocity near the edge is clearly larger than that in the centre.

The corresponding measurements of the velocity across the port at high excitation levels, well past the stage of jet formation and turbulent flow, were 13.5, 13.6, 14.8 and 16.3 m/s. For such flow speeds in a pipe, we would expect the velocity profile to be almost flat, there being only a thin boundary layer where the flow reduces to zero at the edge. But for the hole, the speed again is largest near the edge although the relative variation is less than before.

For a source on an infinite baffle, the acoustic output represents the sum of all the elementary sources, summed over the port opening. Calculation of port acoustic output should take the velocity profile into account, especially to compute the near field response, since a microphone positioned along the baffle will experience an increased output due to the higher velocities near the edge.

The foregoing velocity profiles complicate microphone measurements along the baffle. The acoustic output of a 7.5-cm diameter port was measured by microphones placed respectively at 10, 20, and 40 cm from the centre of the hole along the baffle, at low excitation levels. A 1/r dependence may not be very appropriate so close to the hole, but the measurements are simply related by a scale difference. The 10-cm rms value is 3.02 Pa, while the 20-cm value, 1.32 Pa, is considerably less than half that. The 40-cm measurement along the baffle diagonal gives 0.535 Pa, which is even further away from what is expected from the 1/r law. There is very little contamination of the microphone signals by the cone motion of the driver behind the test box, so the deviation from the 1/r law probably lies in the finite size of the baffle. The diffraction from the edges of the baffle reduces the amplitude as the edge is approached It was impractical to increase the size of the baffle to beyond 4 ft. square.

The dilemma of the experiment just presented is that acoustic measurements of ports should be at least one diameter from the edge of the port, to avoid nearfield effects, yet the finite baffle size makes this problematic. The loudspeaker cabinet may also limit the choice of positions. The other alternative would be to measure at the port mouth, if the theory of the port output were better known. We return to this later.

Fig.9 shows measurements at 10, 20 and 40 cm from the port centre, but at high acoustic levels, well beyond jet formation. The signals now do not even look the same. The figure also shows the jet burst of flow one radius in front of the port, on axis. Notice that the nearest microphone displays an asymmetrical, disturbed signal, largely positive, corresponding roughly to the velocity maximum of the air flow. It is tempting to try to associate the jet plume moving at relatively high speed with a Bernoulli pressure drop $(1/2)\rho v^2$ which might then act as a monopole source. However, its effect would fall off as 1/r, and hence would relatively remain at the same amplitude as the acoustic signal due to efflux of air from the port. This contradicts the microphone data. A companion paper [4] on artefacts of microphones in high-level near-field measurements shows that when a microphone is placed adjacent to the jet stream, a large negative pressure pulse results which is a measure of the

Bernoulli effect. But a microphone along the baffle is too far away for such an effect, and from the graphs it is clear that the corrupting signal is largely positive.

A dipole source can be interpreted as an external force applied to the fluid. This is only possible near a boundary, such as the baffle. Quadruple and higher-order sources, however, can occur in the body of a fluid in violent motion, and they invariably occur in the high-shear layer of air adjacent to the jet plume. These seem appropriate to explain the very sharp spatial response of the signal. Thus we interpret the near-field artefact as pseudo-sound created by the turbulence of the air near the jet column. Such sources may be quadrupoles, whose near-field response falls off at least as fast as $1/r^5$, in contrast to monopoles which have a 1/r falloff, and dipoles whose near-field falls off as $1/r^2$ [5].

A Theory for the Velocity Profile and the Nearfield Pressure

The data of the previous section could not be quantitatively understood, so an effort was made to re-evaluate the theory of acoustic ports. Since many ports are rather short, attention was turned to a simple hole in an infinite baffle.

One way to visualize the flow lines at low levels near a hole in a wall is shown in Fig.10. The diagram shows a cross-section of the lines of an oblate spheroidal co-ordinate system [7,8]. The wave equation is separable in these co-ordinates, and their value is that the boundary conditions for a hole in an infinite, thin baffle are natural in this system. The baffle is drawn in as a thickened line, which is interrupted by the position of the hole. The hyperbolic lines going through the hole represent streamlines of steady airflow, which are automatically tangent to the adjacent baffle, away from the hole. The perpendicular ellipses represent lines of constant acoustic pressure at low frequencies. These lines become spherical far away from the hole, and the perpendicular flow lines are uniformly spaced around a large circle, illustrating that the hole acts like a point source at large distances.

The flow lines converge near the edge, and thus it is clear that the air speed becomes very large there. The velocity profile across the hole is far from uniform! An actual port has a baffle of finite thickness, which tends to reduce these high speeds, but it is probable that the high velocities near the sharp edges caused the instability which was observed by the hot-wire anemometer.

While this low-level flow pattern is unexpected, the high-level situation is even more complex, but is believed to be similar on the intake side of the hole, after the disturbance from the previous half-cycle has subsided. Fig.11 shows the proposed flow pattern during each half-cycle, in which a jet of air is forced away from the hole. The jet has an outward plume (moving to the right in the diagram) with lots of turbulence near the edges, but the air entering the hole is drawn in more uniformly, with flow lines similar to those of the low-level case shown in Fig.10. Hence we expect the air speed near the edge to be larger for high levels as well.

Oblate spheroidal co-ordinates are described by η, where $\eta=\cos(\theta)$, θ being the angle from the z-axis of the streamlines far from the origin; ξ, a variable describing the elliptical contours, which is zero at the hole, and ϕ, the azimuthal angle. The Cartesian co-ordinates x, y, z are related to the foregoing by:

$$\begin{aligned} x &= R\sqrt{[(\xi^2+1)(1-\eta^2)]}\cos(\phi) \\ y &= R\sqrt{[(\xi^2+1)(1-\eta^2)]}\sin(\phi) \\ z &= R\,\xi\,\eta. \end{aligned} \qquad (22)$$

The lines of constant η are the hyperbolas in Fig.10, while the lines of constant ξ are the ellipses. The constant R is the radius of the hole under study, and there is circular symmetry about the z-axis, which passes through the middle of the hole. It is convenient to use $r=\sqrt{(x^2+y^2)}$ as the distance from the z-axis. Note that the positive z-axis is described by $\eta=1$, the negative by $\eta=-1$. On the baffle $\eta=0$, and the variable ξ then describes points on it away from the hole. On the other hand a position in the hole is described by $\xi=0$, and η describes points across it.

The velocity perpendicular to the constant-ξ surfaces is given for $\eta>0$ by [8]:

$$v = [U/(2\,\pi\,R^2)]/\sqrt{[(\xi^2+\eta^2)(\xi^2+1)]}, \tag{23}$$

where U is the volume velocity [m^3/s] through the hole. From this equation we can extract both the velocity profile across the hole, and the velocity of the air along the baffle away from the hole.

At the hole $\xi=0$, and η describes the variation across it. The velocity becomes:

$$v(\eta) = U/(2\,\pi\,R^2\,\eta), \tag{24}$$

and to transform η into the variable r, for $\xi=0$ we have $r=R\sqrt{(1-\eta^2)}$, so that in terms of r, the velocity profile across the hole becomes for $r<R$:

$$v(r) = U/[2\,\pi\,R\sqrt{(R^2-r^2)}]. \tag{25}$$

Note that the air velocity v(r) in the hole becomes infinite at the edge (r=R).

Along the baffle $\eta=0$ the velocity (23) becomes:

$$v = U/[2\,\pi\,R^2\,\xi\sqrt{(\xi^2+1)}], \tag{26}$$

and to convert this to distance r from the hole centre, for $\eta=0$ we have $r=R\sqrt{(\xi^2+1)}$, so that for $r>R$,

$$v(r) = U/[2\,\pi\,r\,\sqrt{(r^2-R^2)}]. \tag{27}$$

Note now that the velocity v(r) tangent to and on the baffle becomes infinite at the edge of the hole (r=R). In (25) above we saw that the air velocity in the hole at its edge was infinite as well! So the air at the edge comes in along the baffle and accelerates to infinite speed as it arrives at the hole, then goes through the hole at the edge, also at infinite speed, and retreats along the baffle on the other side of the hole, with infinite speed just at the edge! Clearly this theoretical prediction will actually be modified by inertial effects, which the present analysis neglects.

Although the above equations are strictly valid for steady flow, we can apply them to a varying acoustic field at very low frequencies, as long as the size of the hole is very small compared to a wavelength. This is true for our experiments and ports in general. Once we know the velocity along the baffle, we can work out the pressure along it as well (or any other streamline) by integrating the density-weighted acceleration from a point r on the baffle to ∞:

$$p(r) = \int_{r}^{\infty} \rho\, j\omega v(r)\, dr = [\rho\, A(t)/(2\,\pi\, R)]\, \sin^{-1}(R/r). \qquad (28)$$

a relatively straightforward relation which asymptotically approaches 1/r for r>>R. Here ρ is the air density, and A(t) is the volume acceleration, which for harmonic time variation is $j\omega U$.

Along the axis of the hole, η=1, and the velocity can be worked out in a manner similar to that of (25):

$$v(z) = U/[2\,\pi\,(z^2+R^2)], \qquad (29)$$

while the pressure along the z-axis becomes:

$$p(z) = [\rho\, A(t)/(2\,\pi\, R)]\, \tan^{-1}(R/z). \qquad (30)$$

Note that p(z) in (30) at z=0 (in the middle of the hole) is the same as the pressure p(r) from (28) for r=R, (at the edge of the hole). In fact the pressure is constant anywhere in the hole on the baffle plane, and has the value $\rho\, A(t)/(4\, R)$. If we think of positive z as outside the hole, then the pressure on the other side, well away from the hole (i.e. inside our box) will be twice the pressure at the hole. At very large distances from the hole, (30) also varies as 1/r (with z as r).

A piston in a baffle does not have a constant pressure over its surface, in contradistinction to the hole discussed here. At the centre of a piston, the pressure is $\rho\, A(t)/[\pi\, R]$, where A(t) is the total volume acceleration defined by its motion. This is higher than at the centre of the hole, but for a piston the pressure at the edge is lower by a factor $2/\pi$. However, the velocity profile of the piston is perforce uniform. Thus while a piston has a flat velocity profile, the hole has a flat pressure profile. The farfield pressure for either (and the velocity) will be the same for the same A(t).

We can think of the air accelerating [at a rate $A(t)/(\pi\, R^2)$] through the hole as a plug of mass M, a so-called *inertance* [8], driven by the total pressure difference, $\rho\, A(t)/[2\, R]$, and find

$$M = \pi^2\, \rho\, R^3\, /\, 2. \qquad (31)$$

How does this inertance compare with that of a customary flanged port of zero length? For such a port the velocity profile is usually assumed to be uniform across the mouth, and the "piston-in-an-infinite-baffle" theory applies. The reactive impedance end correction for the two ends repr: ·ents an inertance of $(16/3)\rho R^3$, which is larger than (31) by a factor 1.081, or 0.675dB. Thus the earlier acoustic output calculations for ports are somewhat too low. If the port has some length, we might expect the velocity distribution to be more uniform, so the inertance of the ends would be intermediate between the two theories. This allows us to close the gap between measured and calculated resonance frequencies for the cosh-shaped port already discussed. Since the inertance of ports is lower than the theory presented first, the calculated resonance frequency should rise, and this will lessen the discrepancy noted earlier.

How does the theory presented above manifest itself in observations? The measured velocity profile of a 10.8-cm hole in a 1.0-cm baffle, at low excitation levels, is shown by the points in Fig.12, superposed with the calculated profile (25). It is clear that the theory applies to the data except very close to the sharp edges, where there may be turbulent activity or flow separation which prevents attainment of the highest speeds. At high levels, the results show a similar trend, and there is no

tendency for the profile to be uniform, as would be the case for flow in a pipe at high Reynolds number.

The variation of measured pressure along the baffle at low level is shown in Fig.13(a), along with a plot of (28), using as normalization the pressure measured at the port centre. The measurements are bit lower than theory, but the trend is correct. Fig.13(b) shows the measured pressure along the port axis at the same level, with a superposed plot of (30), again normalized to the pressure at z=0. Agreement is good, and the finite baffle size may explain the reduction in each case.

The relations (28) and (30) are very important in near-field measurements of ports, especially holes in a baffle, since they apply much better than the customary "piston-in-a-baffle" approach.

The Compression of a Port

It is now perhaps opportune to return to the nonlinear port model, whose calculations did not represent so well the measured pressure outside a hole. Since the velocity profile for a hole is non-uniform, as we have measured, then the model may be significantly in error. For a longer port, though, we might expect the profile to be more uniform, and to that end, a simple cylindrical port of diameter 3.45 cm and length 6 cm was modelled and measured at high level. It has sharp edges on both ends, which may help to promote flow separation and turbulence.

Fig.14 shows the measured box pressure (a), the measured pressure on the baffle 20 cm from the port (b), the modelled 20-cm pressure (c), and the measured throat air speed. The model used a critical velocity of 8 m/s, a transition width of 3m/s, and the acceleration coefficient was reduced by a factor 0.8. Clearly the agreement is now quite good. Even the peak model velocity, which was 18.4 m/s, agrees with the anemometer results. Note that the $(1/2)\rho v^2$ losses cause the velocity to be now more in phase rather than in quadrature with the driving pressure, causing the volume acceleration, and hence the output pressure, to lead the box pressure.

The broad behaviour pattern of loss induced by the jet formation can explain well-known port properties. To make useful calculations, we shall start by making the box pressure an undistorted sine wave, so that both the compression and the distortion of a port can be determined. When drive levels of real systems rise, the box pressure may be distorted due to driver nonlinearity, or the varying acoustic impedance of the port. For our model we use a 7.5-cm diameter port 10 cm long, a critical velocity of 5 m/s, with a transition width of 1 m/s. For other port diameters, the critical velocity may be scaled so that the Reynolds number, $\rho v d/\mu$, stays the same. Thus the product of port diameter and critical velocity should be constant, for a port of a specific shape.

Fig.15 shows the calculated output of the port versus the rms sinusoidal box pressure. There are two curves, the upper one showing the rms level of the fundamental, the other the rms level of all distortion components. It is clear that there is very little compression until the $\rho v^2/2$ loss term sets in, at a box pressure just below 200 Pa rms. Until that point, the distortion is less than 1%. The distortion rises quickly beyond 200 Pa rms, and a gentle compression starts, which reaches 3dB at about 2000 Pa. Beyond these levels, the output goes up roughly as the square root of the box pressure, as expected from (18). The distortion rises somewhat more rapidly than the output, and is about 37% at 10000 Pa rms box pressure. At 20000 Pa rms, the output extrapolated from low levels would have been 450 Pa, whereas the model gives 132. This is a compression of 10.7 dB. In reality,

compression could be higher still, since driver voice coils tend to heat up, and BL products fall at high cone excursion.

An additional aspect of port compression is not immediately apparent from Fig.15. Although the compression seems fairly tame when plotted against box pressure, the losses destroy the Q of the port resonance, and this has a significant effect on the port output. Future work will consider this.

Fig.16 shows the box pressure, output pressure at 20 cm, and the throat velocity of the model for an extremely-high box pressure of 20000 Pa rms. The throat velocity, although not sinusoidal, is almost in phase with the box pressure, and the resulting volume acceleration and output pressure display large spikes. These spikes represent high harmonics, and there is 43% distortion.

The general trend of the calculated data of Fig.15 will apply to most ports, when allowance is made for the different critical velocities and port A/L ratios. The onset of inertial effects may depend somewhat on the detailed contours and surface smoothness of the port, but the main characteristics of the port losses and distortion seem difficult to avoid. If deleterious effects occur in a particular design, the only certain remedy is to increase port area and length so that A/L remains constant This will reduce the velocity in the port for a desired output, and hence reduce inertial effects.

Conclusion

The study of loudspeaker ports is clearly not complete, but in this paper the losses caused by a jet stream have been identified, and model results show the trend of compression and distortion. The measurements and theory of both the velocity profile across a port and the pressure near it are new results which help in the assessment of ports.

Acknowledgements

The author is grateful for support from the Natural Sciences and Engineering Research Council of Canada. Low-frequency drivers for this work were supplied by Cambridge Speakers, Ltd, TGI Ltd., and JBL Inc. Stanley Lipshitz and Jan Abildgaard Pedersen contributed in valuable discussions.

References

1. John Vanderkooy, "Loudspeaker Ports", presented at 103rd AES Convention, New York 1997 Sept. 26-29, preprint #4523.

2. Juha Backman, "The Nonlinear Behaviour of Reflex Ports", presented at 98th AES Convention, Paris 1995 February 25-28, preprint #3999.

3. U.Ingard and H.Ising, "Acoustic Nonlinearity of an Orifice", J. Acoust. Soc. Amer. 42, p.6-17, 1967.

4. Jan Abildgaard Pedersen and John Vanderkooy,"Near-Field Acoustic Measurements at High Amplitudes", presented at 104th AES Convention, Amsterdam, 1998 May 16-19, a companion paper.

5. P.M.Morse and K.U.Ingard, *Theoretical Acoustics*, Princeton University Press, 1968. Reprinted by McGraw-Hill.

6. L.L.Beranek, "*Acoustics*", American Institute of Physics, 1954, 1986.

7. E.Skudrzyk, *The Foundations of Acoustics*, Springer-Verlag, 1971, p.482ff.

8. P.M.Morse and H.Feshbach, *Methods of Theoretical Physics*, Parts I and II, McGraw-Hill, 1953.

Figure Captions

1. Test setup. The driver was mounted on a 25-l test box which had a 4-ft by 4-ft baffle attached to the front, containing the port. Microphones measure the pressure in the box and also outside the port, usually along the baffle.

2. Showing a box containing a port with parameters as indicated.

3. Measurements at 30 Hz for a 7.5-cm hole in a baffle 1.7 cm thick at low levels. Upper curve (a) is box pressure, (b) is output 10 cm from the hole centre along the baffle, (c) is 20 cm away, and (d) is the output of a hot-wire anemometer, placed in the centre of the hole. The output is in phase with the box pressure. The hot-wire probe shows a frequency-doubled output since it responds only to the magnitude of velocity.

4. Showing the same measurements as Fig.3, but at high acoustic levels. The hot-wire anemometer probe has been placed 10 cm from the port, on its axis. The sharp peaks of rapid air flow indicate the formation of a jet from the port.

5. Signals of Fig.4(b) and (c), normalized to the same amplitude, showing the distortion of the nearer signal.

6. Measurements of the air velocity at distances of 1, 2, 3, 5, 10, 15, 20, 30, and 50 cm along the axis of the port. The jet burst of air moves out at about 10 m/s, although the air velocity in it shows peaks of 20 m/s.

7. Longer time records of the air velocity at distances of 50 cm (upper) and 80 cm (lower) from the port characterized in Figs.3-6. The jet or vortex ring has basically collapsed at this range.

8. Comparison of the measured output at 20 cm (upper), at high levels, from a 7.5-cm port in a baffle 1.7 cm thick, with model calculations described in the text (lower).

9. Measurements of a 7.5-cm port at high acoustic levels, at 10 (upper), 20 (upper middle), and 40 cm (lower middle) from the port, along the baffle. The nearest microphone signal is distorted, and the distortion seems related to the measured air velocity 7.5 cm in front of the port (lower). The two furthest pressures look quite similar. The amplitudes do not follow a 1/r-law very well.

10. Visualisation of the flow lines near a hole in a baffle at very low frequencies. The diagram shows the cross-section of an oblate spheroidal co-ordinate system, and the baffle is drawn in as a heavy line. The hyperbolas are lines of constant η, ellipses lines of constant ξ.

11. Drawing of the proposed flow pattern during one half-cycle of the flow from a port at high levels. The jet of air flow may be part of a vortex ring which is cast off by the port. The incoming air has a flow pattern very similar to that of Fig.10.

12. Points show the measured velocity profile of a 10.8-cm hole in a baffle 1.0 cm thick, while the curve shows the calculated theoretical profile. The data is taken at low level, well below jet formation. The point near the edge of the hole falls well below the theory, perhaps because of instability or shadowing created by the sharp edges. At 5.4 cm radius, theory predicts an infinite velocity for a hole in a thin baffle.

13. Pressure along the baffle (a) for a 10.8-cm hole, at low level. The measured points can be compared with the curve for the theory. The trend is correct, but the exact magnitude is not. For measurements along the axis of the port (b), the conformity to theory is a bit better. Both theoretical curves have been normalized by the pressure at the centre of the hole.

14. Calculations and measurement of port output for an overdriven 3.45-cm diameter cylindrical port 6.0 cm long. (a) shows box pressure, (b) pressure at 20 cm along baffle, (c) is the calculated pressure at 20 cm, and (d) is the measured throat velocity. The model agrees fairly well with the measurement.

15. Calculated output of a 7.5-cm diameter port 10 cm long, with a critical velocity of 5 m/s, as a function of rms box pressure driving the port. The upper curve is the fundamental rms output, the lower is the rms output of all the harmonics.

16. Modelled box pressure (a), output at 20 cm (b), and throat velocity (c), for the port described in Fig.15. The throat velocity is essentially in phase with the box pressure, which makes the port losses high. Such losses would severely lower the Q of the port resonance, and this needs to be taken into account in the operation of a loudspeaker system.

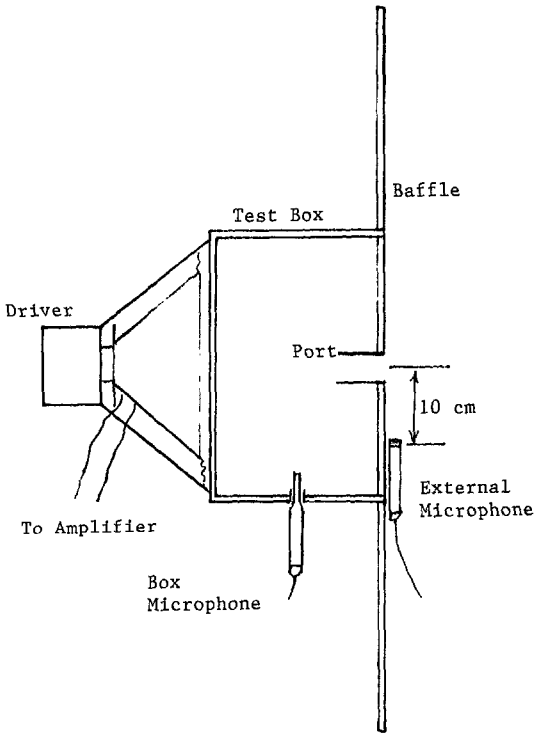

Figure 1

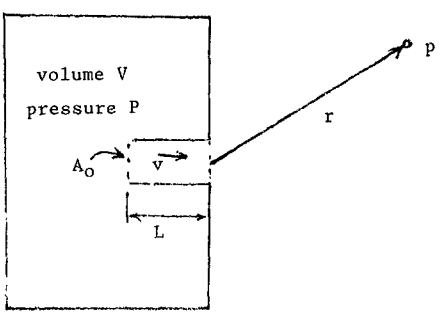

Figure 2

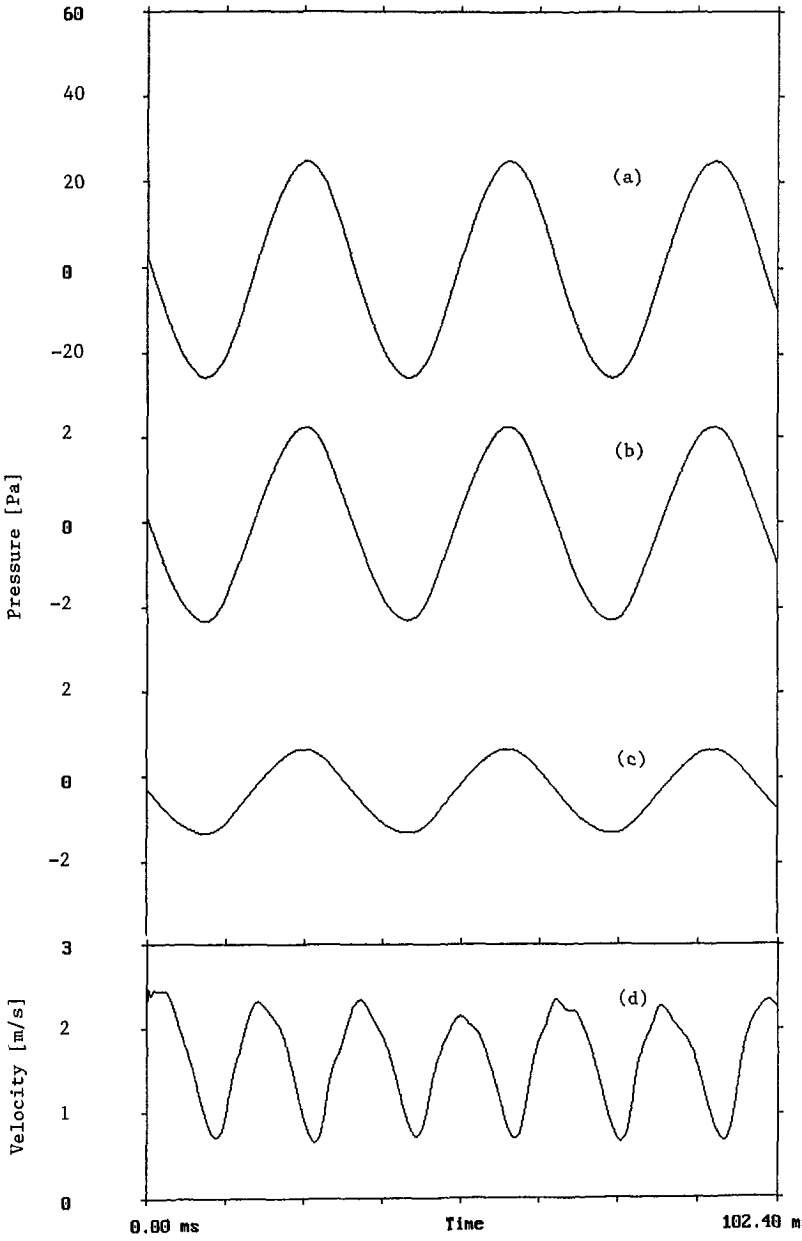
60
40
20
0
-20
2
0
-2
2
0
-2
3
2
1
0
Pressure [Pa]
Velocity [m/s]
(a)
(b)
(c)
(d)
0.00 ms
Time
102.40 ms

Figure 3

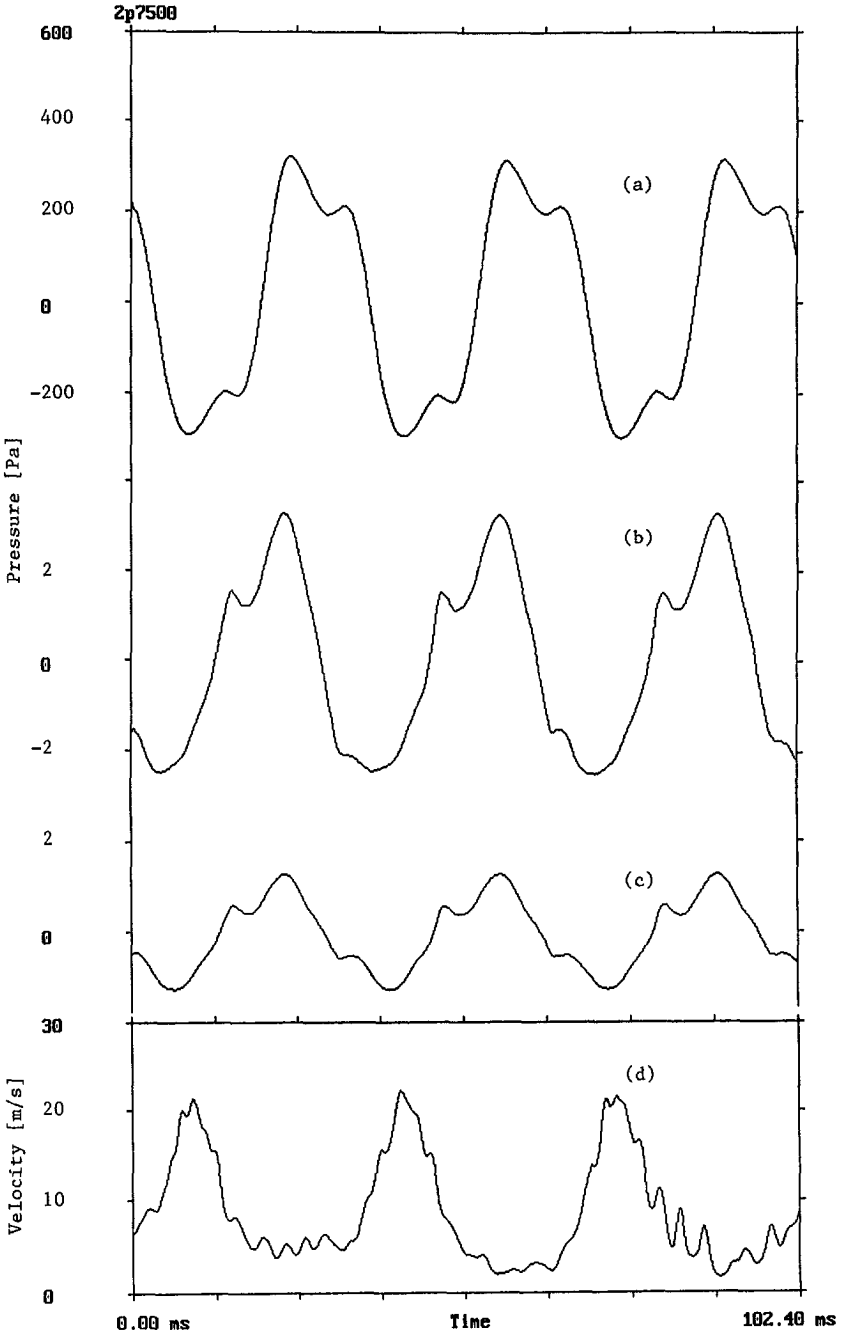
2p7500
600
400
200
0
-200
Pressure [Pa]
(a)
2
0
-2
(b)
2
0
(c)
30
20
10
0
Velocity [m/s]
(d)
0.00 ms
Time
102.40 ms

Figure 4

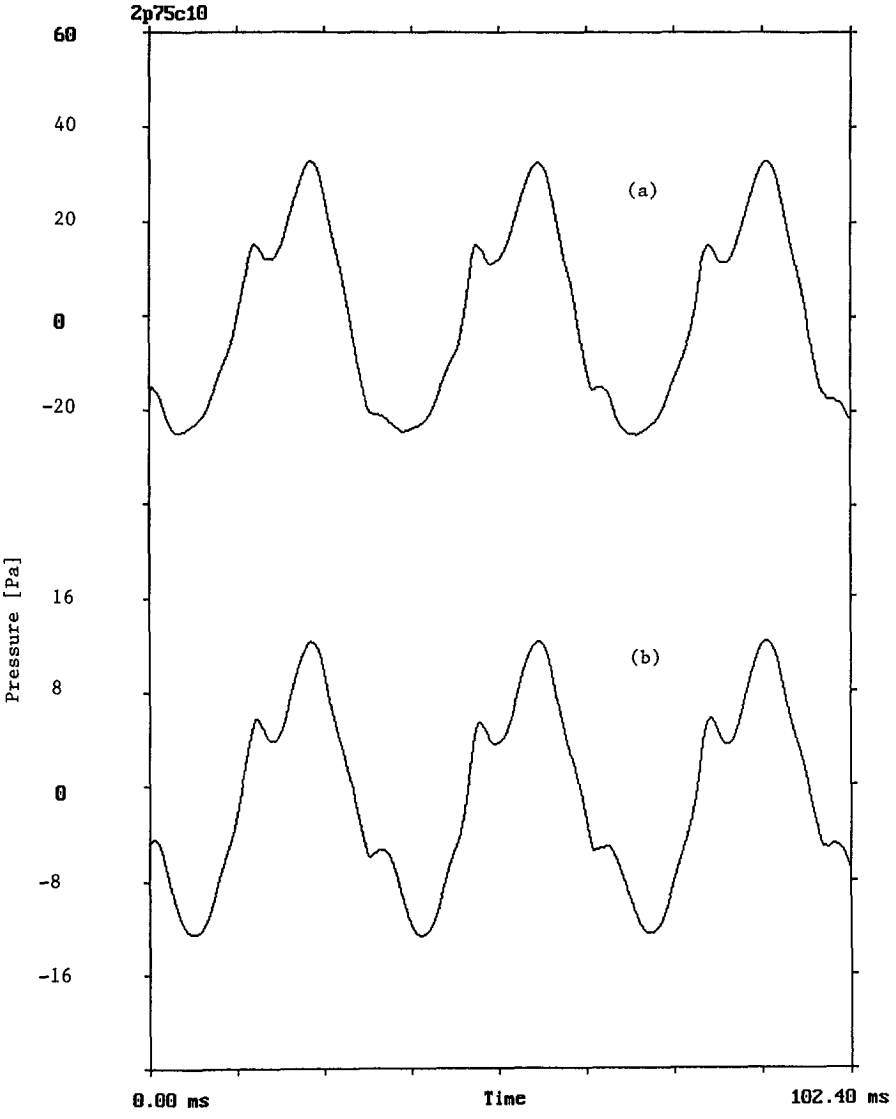
2p75c10
60
40
20
0
-20
(a)
16
8
0
-8
-16
(b)
Pressure [Pa]
0.00 ms
Time
102.40 ms

Figure 5

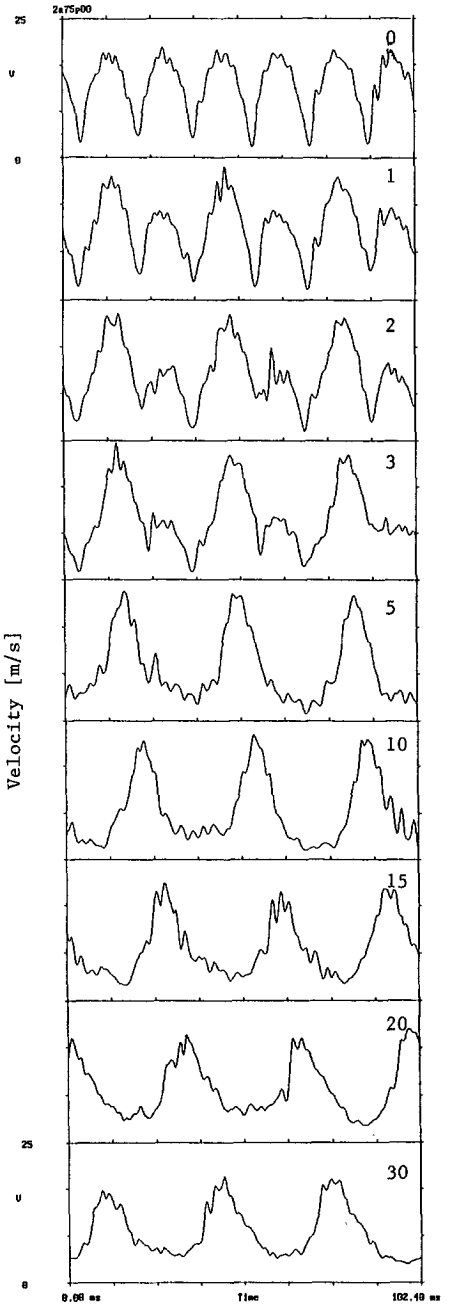
2a75p00
25
0
0
1
2
3
5
10
15
20
25
30
0
Velocity [m/s]
0.00 ms
Time
102.40 ms

Figure 6

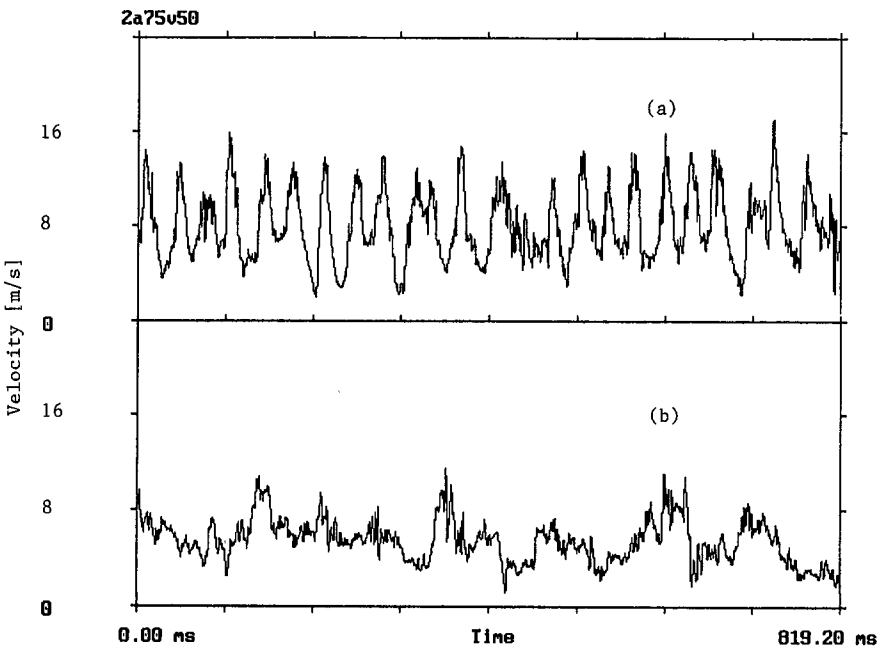

Figure 7

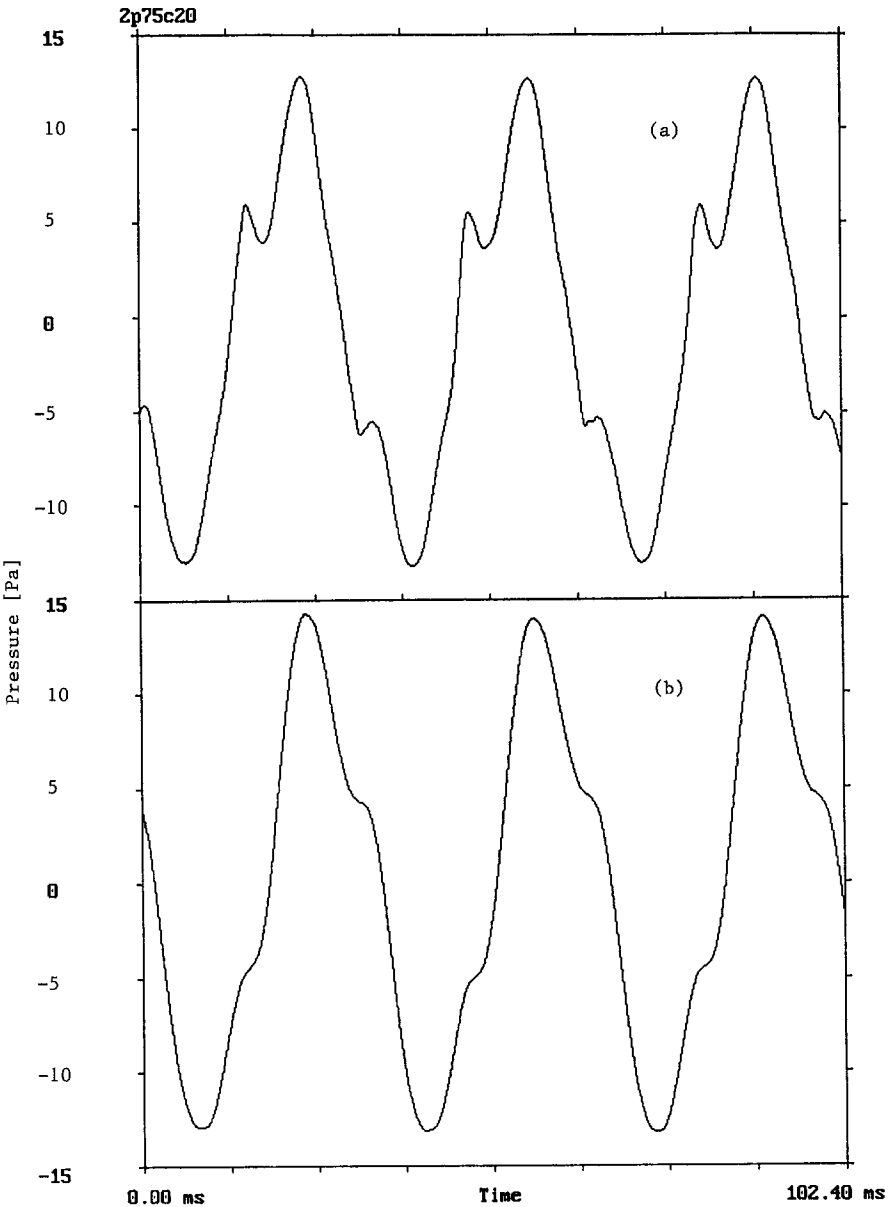
2p75c20
15
10
5
0
-5
-10
(a)
15
10
5
0
-5
-10
-15
(b)
Pressure [Pa]
0.00 ms
Time
102.40 ms

Figure 8

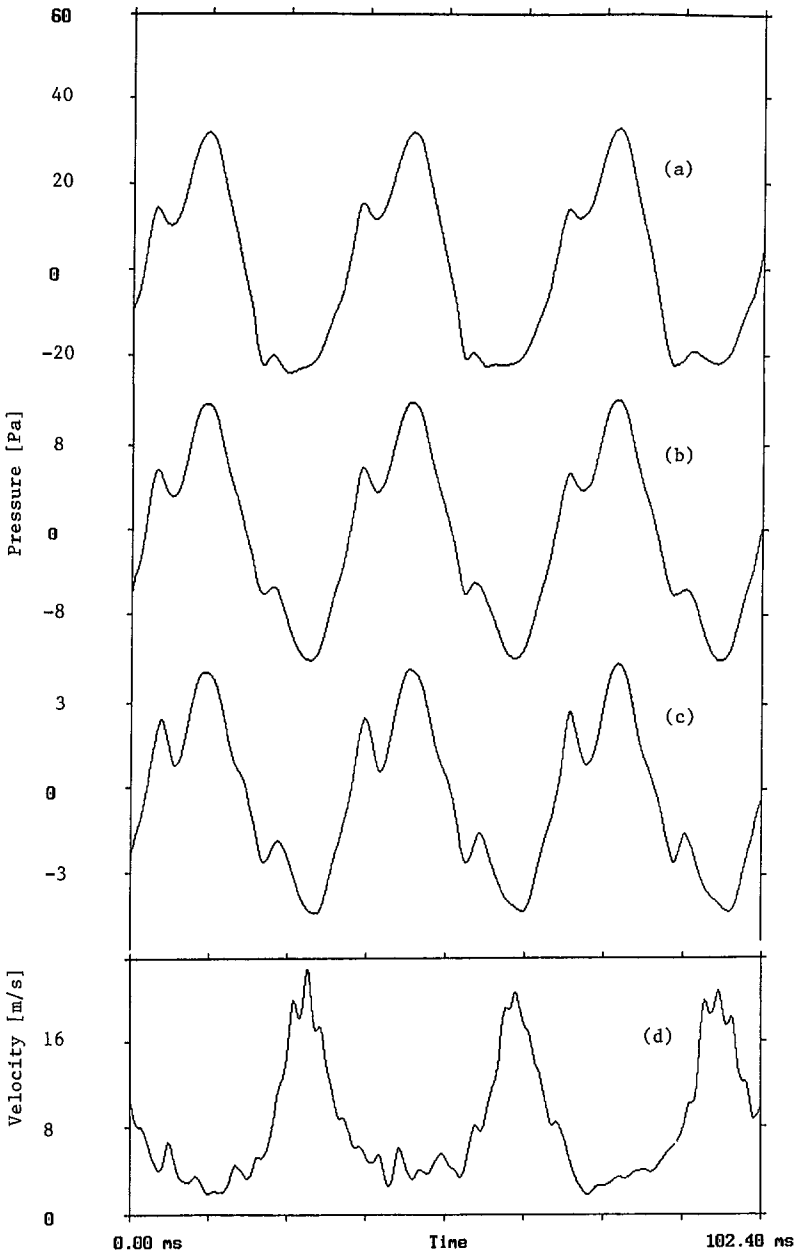
60
40
20
0
-20
8
0
-8
3
0
-3
Pressure [Pa]
(a)
(b)
(c)
(d)
Velocity [m/s]
16
8
0
0.00 ms
Time
102.40 ms

Figure 9

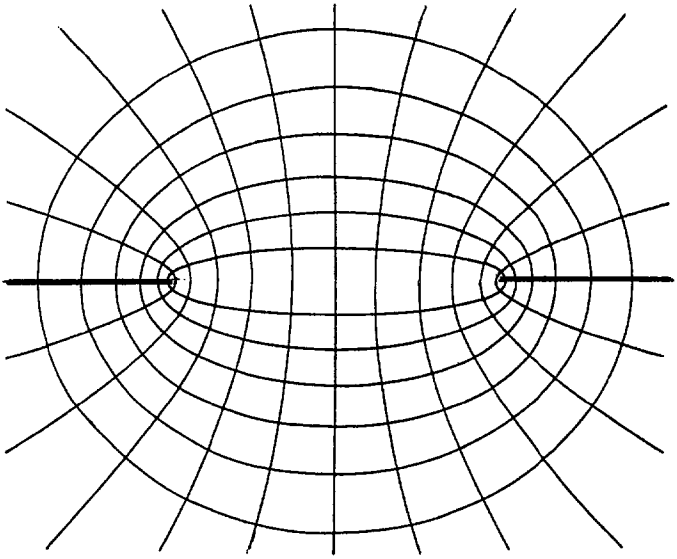

Figure 10

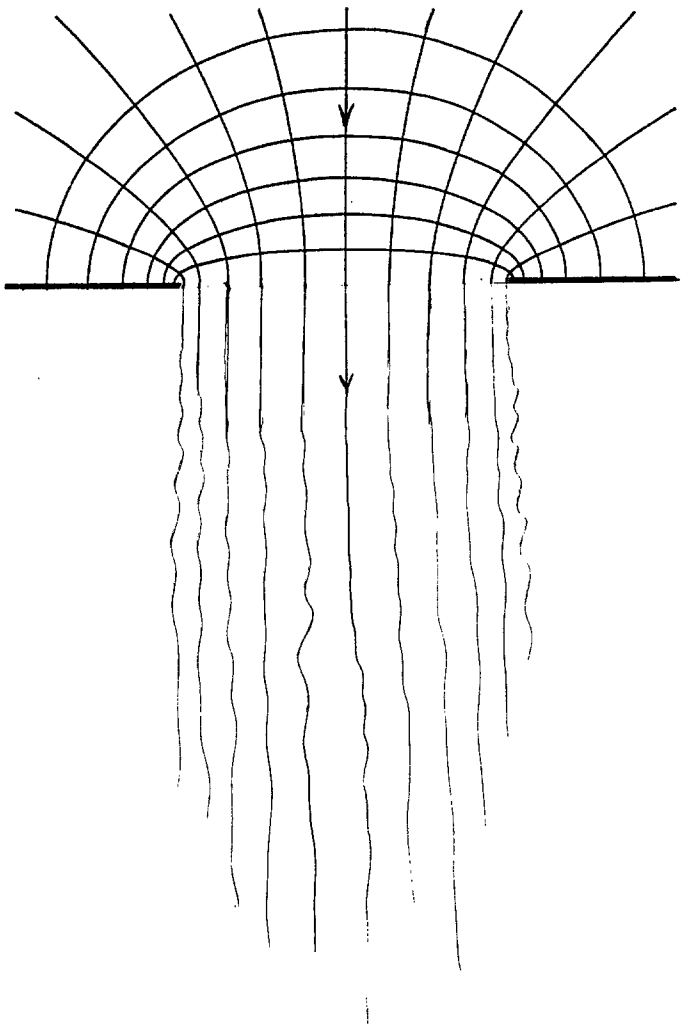

Figure 11

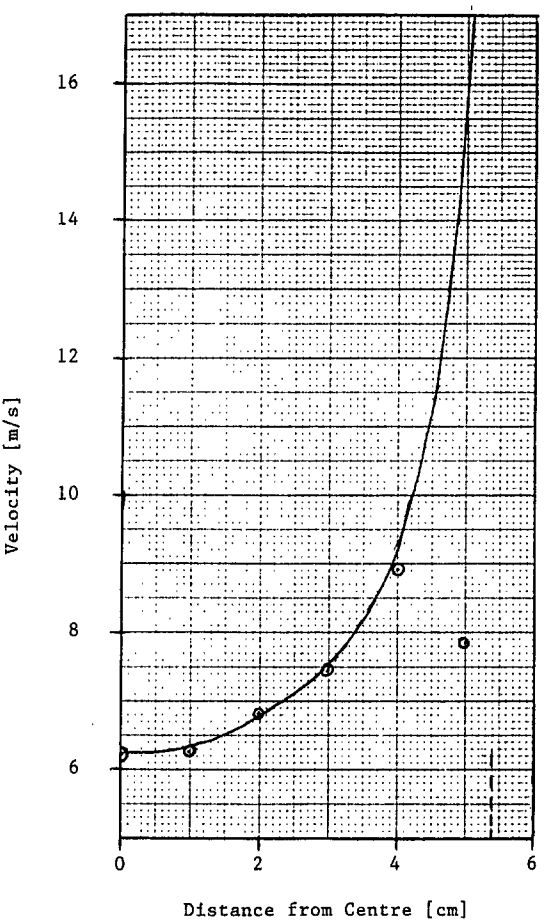

Figure 12

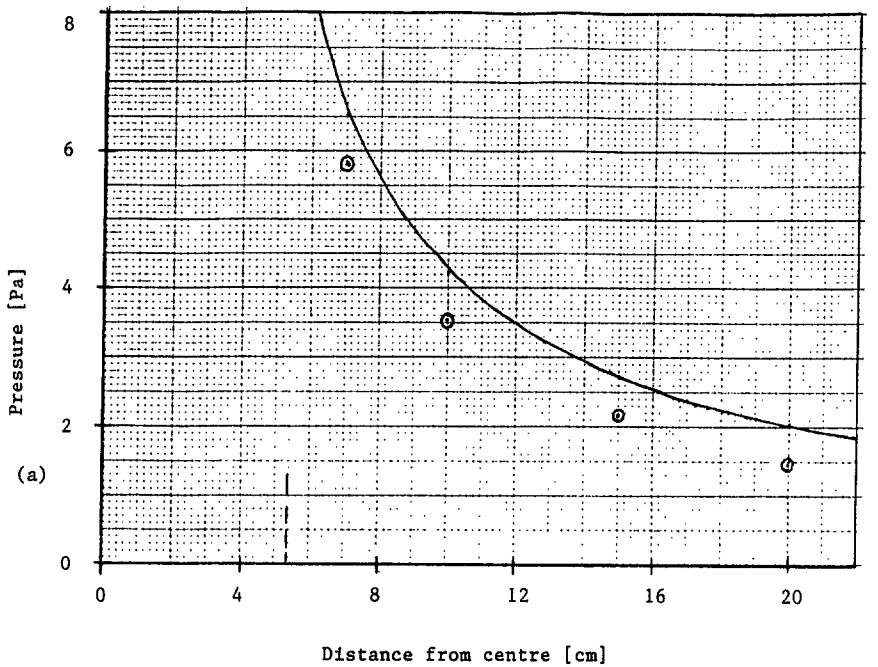
Pressure [Pa]
(a)
0
2
4
6
8
0
4
8
12
16
20
Distance from centre [cm]

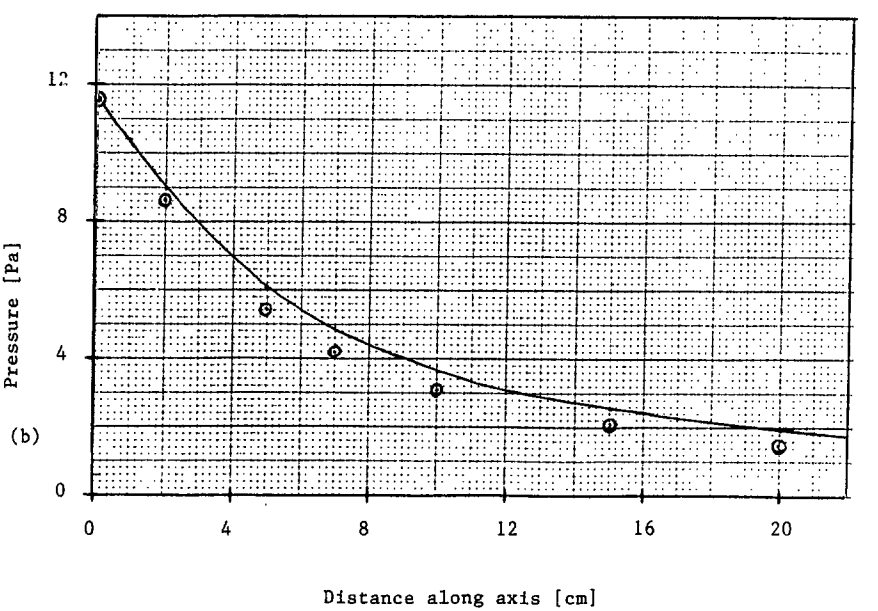
Pressure [Pa]
(b)
0
4
8
12
0
4
8
12
16
20
Distance along axis [cm]

Figure 13

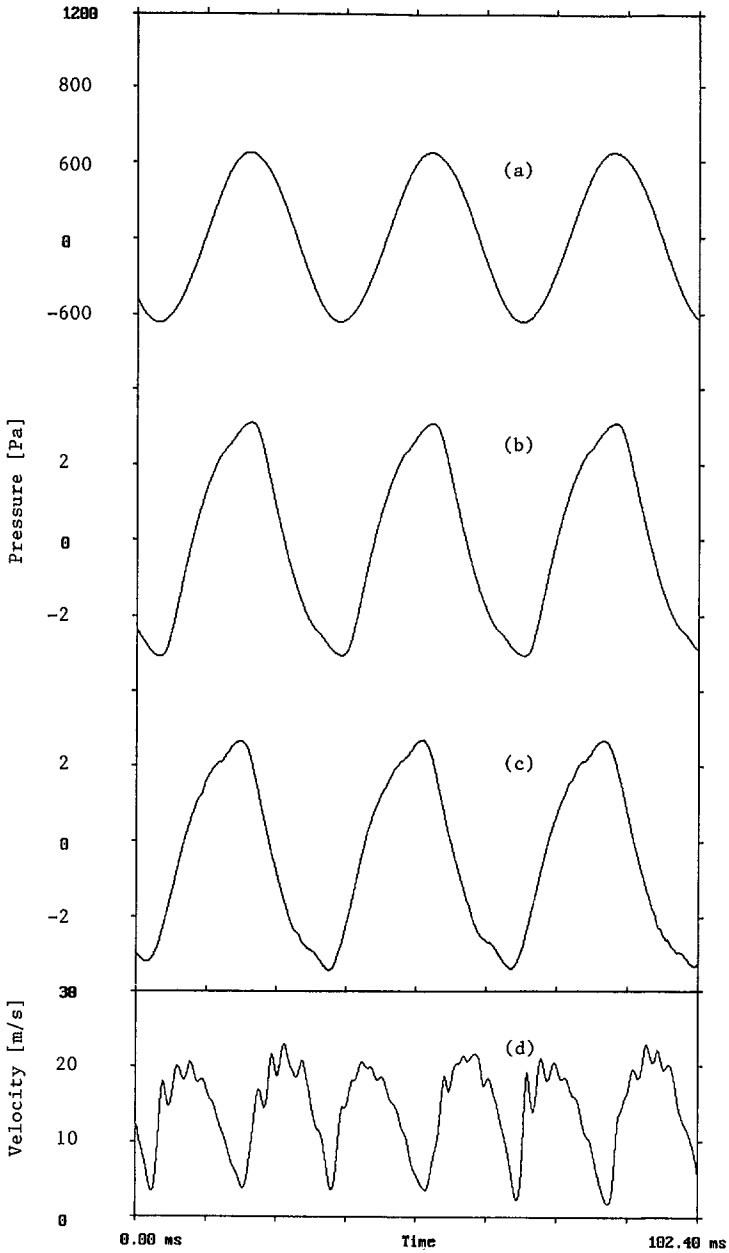
1200
800
600
0
-600
(a)
Pressure [Pa]
2
0
-2
(b)
2
0
-2
(c)
30
20
10
0
Velocity [m/s]
(d)
0.00 ms
Time
102.40 ms

Figure 14

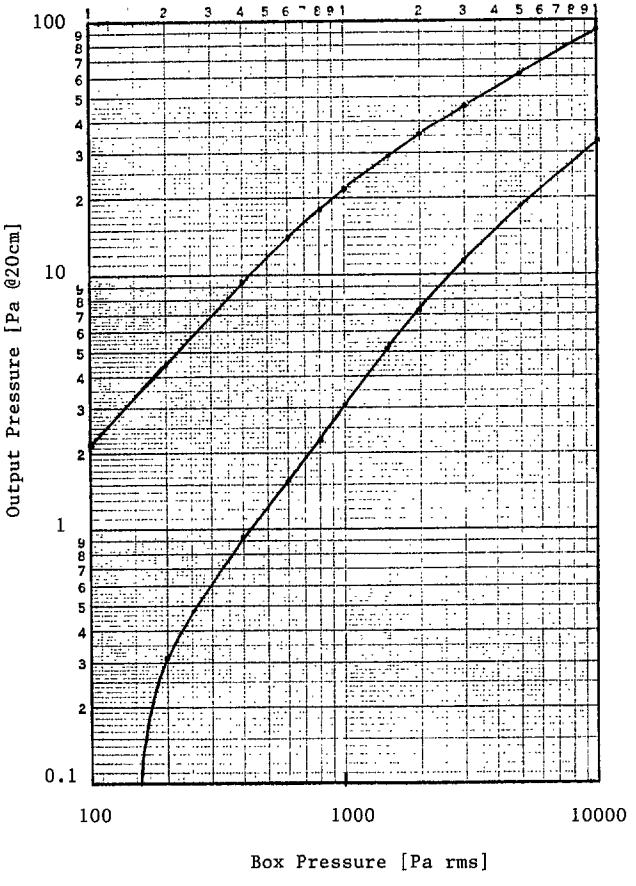
Output Pressure [Pa @20cm]
100
10
1
0.1
100
1000
10000
Box Pressure [Pa rms]

Figure 15

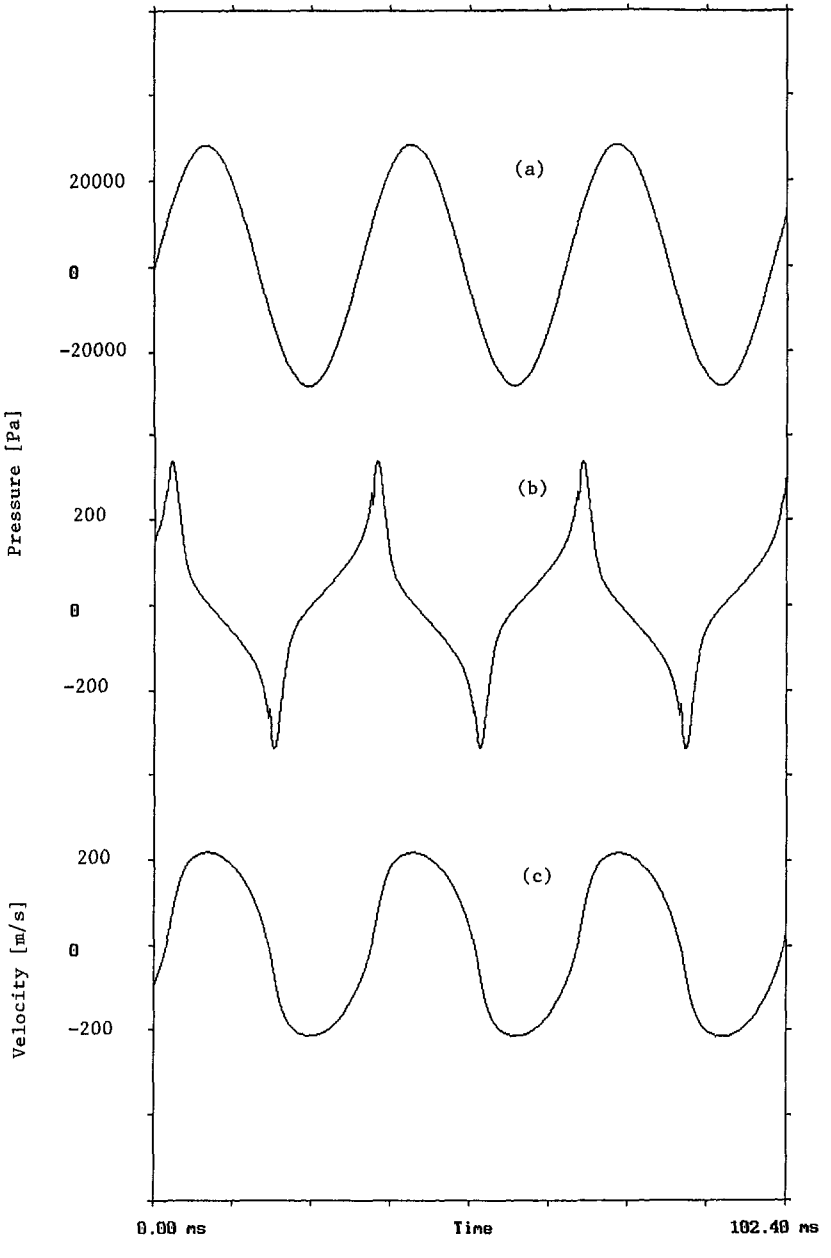
20000
0
-20000
(a)
Pressure [Pa]
200
0
-200
(b)
200
0
-200
(c)
Velocity [m/s]
0.00 ms
Time
102.40 ms

Figure 16